Nuclear Data for Science and Technology (1988 MITO), 275- 278, Copyright © 1988 JAERI.

DIFFERENTIAL CROSS SECTIONS FOR GAMMA-RAY PRODUCTION BY 14 MeV NEUTRONS WITH SEVERAL ELEMENTS IN STRUCTURAL MATERIALS

Isao Murata, Junji Yamamoto and Akito Takahashi

Department of Nuclear Engineering, Osaka University
2-1 Yamada-oka, Suita, Osaka 565, Japan

Abstract: Energy differential cross sections for the gamma-rays produced from the (n,xγ) reactions by 14 MeV neutrons were measured in the gamma-ray energy range from 700 keV to 10 MeV using an NaI spectrometer. Results were obtained for the 8 natural elements; C, Al, Si, Cr, Fe, Ni, Cu and Mo. For prominent discrete gamma-rays in the differential cross sections, the production cross sections were determined by measuring angular distributions with a Ge detector. The gamma-ray energy covered the range between 500 and 3000 keV. The energy distributions have been compared with the differential cross sections evaluated in the nuclear data files of JENDL-3T, ENDL and ENDF/B-IV. The evaluations in JENDL-3T agreed fairly well with the measurements concerning the continuum energy spectra for secondary photons. Discrepancies appeared, however, for Si, Cr and Ni at the energies where the discrete gamma-rays were dominant. The ENDL evaluations were largely deviated from the experimental data. The production cross sections for the discrete gamma-rays in ENDL and ENDF/B-IV were available for the comparison with some of the measured cross sections. Results are presented for C, Al and Si.

(gamma-ray production, 14 MeV neutron, differential cross section, secondary photon energy distribution, discrete gamma-ray, angular distribution, nuclear data file)

Introduction

Nuclear data for gamma-ray production are of primary interest in the neutronics studies for D-T fusion reactors in order to calculate the total radiation field produced by the interaction with the D-T neutrons. Requirement for the experimental data has been given not only for the production cross sections but also for the secondary photon energy distributions. It is also necessary to accumulate the data for prominent discrete gamma-rays in the energy distributions. The present work has been initiated to provide these experimental data by measuring systematically both of the energy differential cross sections and the production cross sections for some discrete gamma-rays emitted from the 14 MeV neutron induced-reactions. Samples were carbon, aluminum, silicon, chromium, iron, nickel, copper and molybdenum, which are of interest as the elements included in the structural materials for fusion reactors.

Many measurements of gamma-ray production cross sections have been carried out /1,4/ at extensive neutron energies, especially around 14 MeV where a number of data have been presented since the D-T neutrons are widely available for many investigators. However, the uncertainties for the energy differential data still remain in the high gamma-ray energy region due to the poorness in counting statistics and energy resolution. One of the objectives of the present experiment is to obtain the differential data with good accuracy in the energy region higher than that where the discrete gamma-rays are dominant. The present production cross sections for the discrete gamma-rays were obtained by a method to measure angular distributions over many gamma-ray emission angles, instead of a conventional method in which the production cross sections are deduced from the differential data measured at a single angular point.

The experimental data are utilized for the verification of the gamma-ray production data evaluated in the current nuclear data files. The energy differential cross sections are compared with the evaluations in JENDL-3T /5/, which is a temporary file for JENDL-3 /6/ and is served for various benchmark tests before the release of JENDL-3. The differential data in ENDL /7/ and ENDF/B-IV /8/ are also available for the present comparison.

Experimental procedure

The experiment has been carried out using the pulsed 14 MeV neutron source of the OKTAVIAN facility of Osaka University /9/. The neutron source is capable of generating 1 x 10^3 neutrons in average per a pulse by bombarding a 10 Ci TiT target with the D^+ pulsed beam of 243 keV. The neutron pulse width was 3 nsec and the repetition frequency was 2 MHz. Energies and intensities of the D-T neutrons had been already examined /10/ as a function of emission angle. The energy spectra have been measured with respect to the D-T neutrons and the gamma-rays produced at the target support by the nonelastic scattering of the D-T neutrons. These data were used for correcting measured cross sections in the data reduction.

Discrete gamma-rays measurement

The gamma-ray energies between 500 and 3000 keV were analyzed with a 180 cm^3 Ge detector. A side view of the experimental layout is schematically shown in Fig.1. The detector is set up in a shield of lead, paraffin, concrete and so on. In order to use the D-T neutrons with a emission angle of 90 deg to the D^+ beam direction, a sample is positioned on the extended line of the detector axis below the neutron source. Seven angles from 30 to 150 deg in the laboratory system were chosen between the emission gamma-rays and the incident neutrons. The energy of incident neutrons was 14.1 MeV ± 170 keV. Time spectra from the sample as well as pulse height spectra (PHS) were measured by means of a time of flight technique to reduce the backgrounds of scattered neutrons from the sample, room-returned neutrons and gamma-rays. The measurements of PHS for the background were made simultaneously with the sample-in runs. Another background run was done without the sample.

The samples are hollow cylinders of 30 mm-

o.d. x 26 mm-i.d. x 70 mm-long. Only for aluminum, the wall thickness is 5 mm. The silicon sample is a 25 mm-diam x 50 mm-long right cylinder. The detector efficiencies for the full energy gamma-ray peaks could be determined using the radioactive sources of ^{137}Cs, ^{60}Co, ^{22}Na, ^{24}Na, ^{56}Mn and ^{57}Ni. Some of the sources have been produced by the irradiation with the 14 MeV intense neutron source. Corrections for the neutron multiple scattering and attenuation in the sample were done with a transport code by a Monte Carlo method. The gamma-ray attenuation was also corrected with this code as functions of the gamma-ray energy and the emission angle from the sample.

The relative yield of the neutron source was monitored by an NE213 liquid scintillation counter, which was located 4 m from the target at zero deg to the D^+ beam direction. The number of D-T neutrons were counted by setting a window within the 14 MeV neutron peak area in the TOF spectrum from the direct source, with a pulse shape discrimination between the neutrons and gamma-rays. The monitor counts were calibrated with the absolute neutron fluences, which were measured by the induced activities in aluminum and niobium foils irradiated with the neutron source.

The statistical errors for individual discrete gamma-ray peaks were 1 to 7 %. Uncertainties in the peak efficiencies of the Ge detector were estimated to be 4.5 % for the energy up to 1.3 MeV and 6.0 % for the energy greater than 1.3 MeV. The errors associated with the neutron flux determination were 7 to 10 %.

Energy distribution measurement

A spectrometer was an NaI crystal of 12.7 cm in diameter and 12.7 cm in length. As shown in Fig.2, the gamma-ray spectra from the sample were observed at a forward direction (45 deg) or a backward one (either 125 or 135 deg). The D-T neutron monitor and the discrimination of the background from the desired prompt gamma-rays were performed in the same manner as those described in the previous section. The sample are pure elemental disks of 10 cm-diam and 5 mm-thick except a silicon sample and a iron one. The distance between the neutron source and the sample was long enough to separate by the flight time the prompt gamma-rays from the gamma-ray background, which were generated at the neutron source and then detected after the scattering in the sample. In the response functions of the NaI detector, the ratios of the full energy peaks to the Compton components could be improved by suppressing the Compton scattering with a collimator of lead placed in front of the detector. For example, the ratio for 6.1 MeV gamma-rays was 11.3 with the collimator and 5.8 without one, respectively.

The measured pulse height spectra were unfolded with the FERDOR code /11/, as well as with another code which was developed in the OKTAVIAN facility. The difference in two unfolded energy spectra was found in the high energy region, where oscillations appeared in the FERDOR spectra. The calculated response functions were used in the unfolding process. The calculated response functions and full energy peak efficiencies have been checked using the measured ones in the energy range from 660 keV to 7.1 MeV and then confirmed to be in good agreement. /12/

The corrections for the multiple scattering and the attenuation of the incident neutrons as well as the produced gamma-rays have been done using a neutron and photon Monte Carlo transport code MCNP /13/. The error estimation for the neutron flux measurements is the same with that in the Ge runs. The errors in the unfolded spectra include the uncertainties of the counting statistics and the response functions of the NaI spectrometer.

Result and comparison with evaluation

The energy differential cross sections for silicon, nickel and molybdenum are shown in Figs. 3 to 5, respectively, and the other cross sections have been given elsewhere /12/. The measurements are compared with the differential cross sections which were derived from the nuclear data for photon multiplicities, transition probabilities, reaction cross sections and secondary photon energy distributions in the evaluated files. The re-evaluation (or modification) years given in ENDL are listed in Table 1 concerning the production cross sections and the secondary photon energy distributions. An original version of JENDL-3T was released in 1987 and no modification has however been made for the file in use.

Silicon pieces were contained within a laminate aluminum case of which wall thickness was 0.1 mm. Due to the low density of this sample, the thickness was nearly equivalent to 5 mm for a natural solid silicon sample. In the unfolded spectrum shown in Fig. 3, the discrete gamma-rays can be observed up to the high gamma-ray energy. The energy differential cross section reproduced from JENDL-3T was roughly comparable to the measured one, but the underestimation of the evaluation was found at the discrete gamma-ray energies of 1, 1.8, 2.8, 4.5, 5 and 7 MeV. In the investigation using the Ge detector, the peak

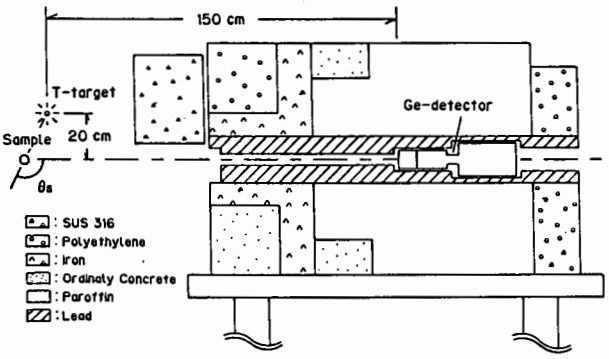

Fig.1. Experimental arrangement for Ge run.

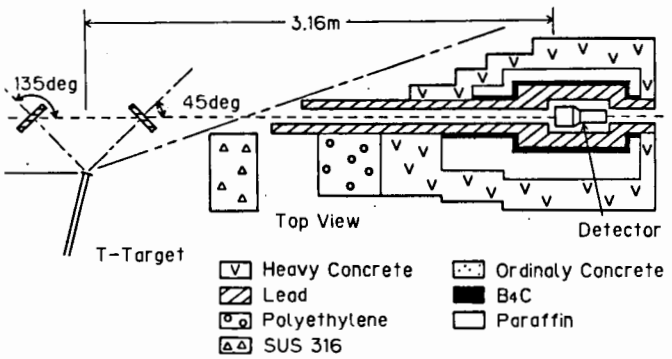

Fig.2. Experimental arrangement for NaI run.

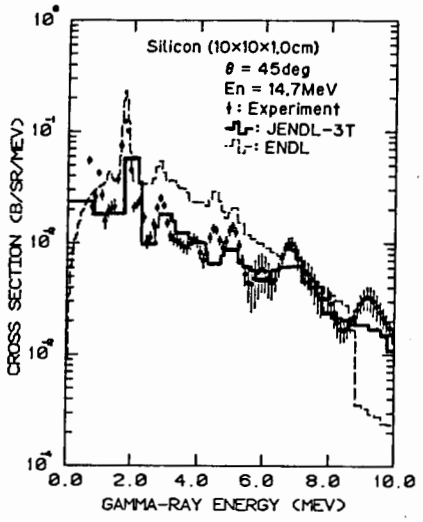

Fig.3. Energy spectra for Si.

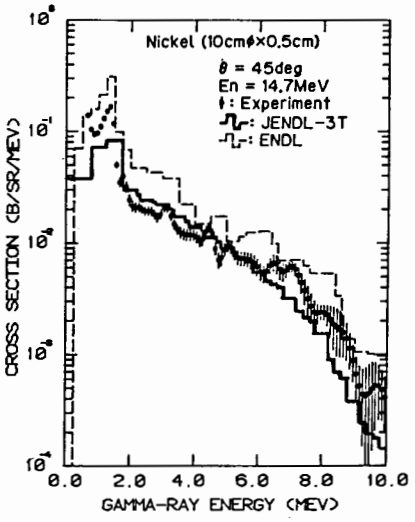

Fig.4. Energy spectra for Ni.

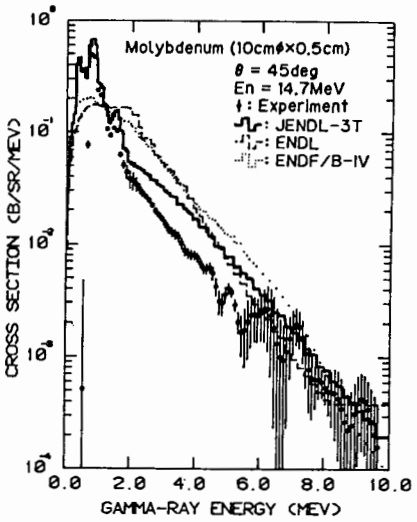

Fig.5. Energy spectra for Mo.

around 1 MeV could be separated into the two gamma-ray lines of $E\gamma$ =941 and 974 keV, of which probable reactions are $^{28}Si(n,p)^{28}Al$ and $^{29}Si(n,n'p)^{28}Al$. The probable reactions for the two discrete lines of $E\gamma$ =1776 and 2831 keV are $^{28}Si(n,n')^{28}Si$ and $^{29}Si(n,2n)^{28}Si$. The differential cross sections in ENDL overestimate the measurements by the factor of 2 in the energy range from 1 to 5 MeV. The ENDF/B-IV evaluation was in good agreement with the measurement. /12/

Figure 4 shows the comparison for natural nickel. The data in JENDL-3T are quite small in the energy range of 1 to 2 MeV, where the discrete gamma-rays appear prominently. For these peaks, it can be identified by the Ge runs that the lines of $E\gamma$ =1331 and 1453 keV have relatively large cross section values of 159 ± 13 and 184 ± 16 mb, respectively. $E\gamma$ =1331 and 1453 keV are ascribed as the respective decays in ^{60}Ni by $^{60}Ni(n,n')$ and in ^{58}Ni by $^{58}Ni(n,n')$.

In the case of natural molybdenum, the production cross sections for fifteen discrete gamma-rays could be obtained by the Ge runs in the energy range of 500 to 1600 keV. As shown in Fig.5, these gamma-rays are taken into account for the photon energy distributions in JENDL-3T. However, large discrepancies between the measurement and the evaluations in ENDL and ENDF/B-IV appear in this energy region. The continuum spectra in all the evaluations overestimate the measured spectra in the energy region between 2 and 6 MeV.

Table 1 lists the production cross section values obtained from the integration of the energy differential cross sections over the range from 700 keV to 10 MeV, for every measured element. The smaller integrated values in JENDL-3T than the measurements for silicon and chromium are due to the underestimation of the cross sections for the discrete gamma-rays at the energies below 3 MeV. The production cross sections in ENDL have larger values than the measured ones for most of the elements. The ENDF/B-IV data are in fairly good agreement with the present experimental values for aluminum, silicon and nickel.

Figure 6 shows angular distributions of the discrete gamma-rays for natural copper. The plotted data for the discrete lines of 1173 and 1861 keV are fitted with the Legendre polynomials using the least-squares method. The energies

Table 1. Energy-integrated production cross sections.

Sample	Cross section (barn) Experiment	JENDL-3T	ENDF/B-IV	ENDL (IO=0, IO=4)
Aluminum	1.22±0.05	1.32	1.39	2.23 ('83, '73)
Silicon	1.53±0.06	1.24	1.53	2.57 ('73, '73)
Chromium	2.27±0.09	1.47	3.88	4.01 ('82, '78)
Iron	2.07±0.09	2.73	2.43	3.40 ('82, '82)
Nickel	2.24±0.10	1.97	2.43	4.30 ('82, '75)
Copper	2.12±0.09	2.53	3.97	2.86 ('82, '78)
Molybdenum	3.37±0.14	4.89	4.30	4.62 ('82, '78)

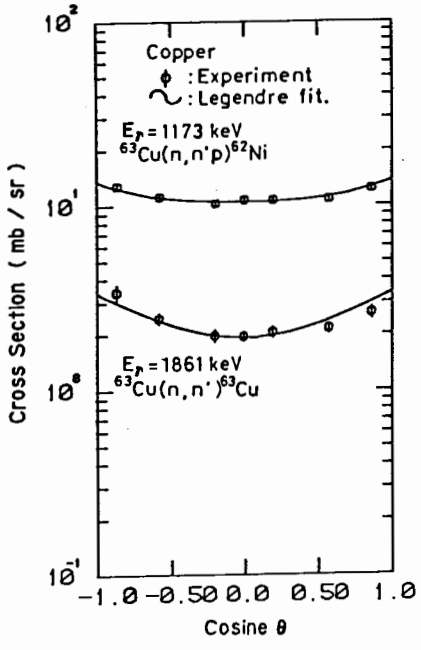

Fig.6. Angular distributions for Cu.

Table 2. Production cross sections for discrete gamma-rays.

Sample	Measured γ energy(keV)	Probable reaction	and transition	Cross Section (mb) Present Exp.	Evaluation ENDF/B-Ⅳ	Evaluation ENDL	
C	4439	$^{12}C(n,n')^{12}C$	$2^+(4439)\rightarrow 0^+(0.0)$	180±7		233	169.3(JENDL-3T) 185.4(ENDF/B-Ⅴ)
Al	844	$^{27}Al(n,n')^{27}Al$	$1/2^+(844)\rightarrow 5/2^+(0.0)$	26±2	41.0	76.8	
	955	$^{27}Al(n,p)^{27}Mg$	$5/2^+(1940)\rightarrow 3/2^+(985)$	15±2	18.5		
	985	$^{27}Al(n,p)^{27}Mg$	$3/2^+(985)\rightarrow 1/2^+(0.0)$	24±2	15.5		
	1014	$^{27}Al(n,n')^{27}Al$	$3/2^+(1014)\rightarrow 5/2^+(0.0)$	60±5	93.0	122.9	
	1698	$^{27}Al(n,p)^{27}Mg$	$5/2^+(1698)\rightarrow 1/2^+(0.0)$	26±3	25.7		
	1808	$^{27}Al(n,n'p)^{26}Mg$	$2^+(1808)\rightarrow 0^+(0.0)$	142±12	119.3	57.0	
	3003	$^{27}Al(n,n')^{27}Al$	$9/2^+(3003)\rightarrow 5/2^+(0.0)$	88±8	96.4	84.9	
Si	585	$^{28}Si(n,\alpha)^{25}Mg$	$1/2^+(585)\rightarrow 5/2^+(0.0)$	36±3			
	941	$^{28}Si(n,p)^{28}Al$	$0^+(974)\rightarrow 2^+(33)$	9±1			
	974	$^{28}Si(n,p)^{28}Al$	$0^+(974)\rightarrow 3^+(0.0)$	24±2			
	1776	$^{28}Si(n,n')^{28}Si$	$2^+(1776)\rightarrow 0^+(0.0)$	310±25		510	474.7(BROND)
	2831	$^{28}Si(n,n')^{28}Si$	$4^+(4608)\rightarrow 2^+(1777)$	48±5		62.5	74.5(BROND)

of $E\gamma$ =1173 and 1861 keV correspond to the excited energies in ^{62}Ni by $^{63}Cu(n,n'p)$ and in ^{63}Cu by $^{63}Cu(n,n')$, respectively. The differential cross section for 1173 keV seems to be nearly isotropic. The angular distributions for low energy gamma-rays may become isotropic in the case where the incident neutron energy is high, since the cascade gamma-ray transitions dominate in the population of levels, compared with direct neutron excitation. The cross section for $E\gamma$ =1861.0 keV has, however, angular dependence.

Table 2 shows the production cross sections for carbon, aluminum and silicon. The data were obtained by integrating the fitted curves with the Legendre polynomials over the emission angles. The carbon data were measured using the experimental arrangement as shown in Fig.2 with the hollow cylinder of 40 mm-o.d. x 15 mm-i.d. x 50 mm-long. The incident neutron energies for carbon were, therefore, different from the other measurements. The cross section value for the 4.44 MeV inelastic level is fairly close to the evaluation in ENDF/B-Ⅴ /14/. In the aluminum runs, the fifteen discrete lines having the energies between 800 and 3000 keV were observed and portions of these lines are compared with the values in ENDL and ENDF/B-Ⅳ. For silicon, the gamma-ray energy covered the range from 569 to 2831 keV. The cross sections in ENDL for $E\gamma$ =1776 keV overestimated the measurement by 65 % and for $E\gamma$ =2831 keV by 30 %, as discussed with the energy distributions shown in Fig.3.

Summary

The energy differential cross sections at the specific angular points were obtained in the energy range from 700 keV to 10 MeV with good counting statistics using the NaI detector. For the discrete gamma-rays which were prominent in the energy differential data, the production cross sections were determined from the angular distributions for the gamma-ray lines separable with the Ge detector.

In the comparison of the secondary photon energy distributions between the measurements and the evaluations in JENDL-3T, no large discrepancies were found in the continuum spectra. The production cross sections should be, however, re-evaluated for the discrete gamma-rays due to no evaluations or underestimations in JENDL-3T for silicon, chromium and nickel. The production cross sections in ENDL overestimated the measurements, although the secondary photon spectra were comparable to the measured ones for aluminum, silicon, iron and nickel.

Acknowledgments

The authors would like to express their gratitude to Prof. K.Sumita for his encouragement, and to Messrs. T.Kanaoka, H.Sugimoto, J.Datemichi and S.Yoshida for their assistance in this experiment.

REFERENCES

1. J.K. Dickens, et al.: Nucl. Sci. Eng. 62, 515(1977)
2. V.C. Rogers, et al.: Nucl. Sci. Eng. 62, 716(1977)
3. Y. Hino, et al.: J. Nucl. Sci. Technol. 15, 85(1978)
4. D.M. Drake, et al.: Nucl. Sci. Eng. 65, 49(1978)
5. JENDL Compilation Group (Nuclear Data Center, JAERI): JENDL-3T, private communication (1987)
6. T. Asami: JAERI-M 87-025, 1(1987)
7. LLNL Nuclear Data Libraries: private communication from R.J. Howerton (1986)
8. ENDF/B summary documentation, BNL-NCS-17541, 2nd Edition (1975)
9. K. Sumita, et al.: Fusion Technology 1982, Vol.1, 675(Pergamon Press 1983)
10. J.Yamamoto, et al.: OKTAVIAN report A-8305, Osaka University(1983)
11. H. Kendrick, et al.: GA-9882, Gulf Radiation Technology(1970)
12. J. Yamamoto, et al.: JAERI-M report 88-065), (NEANDC(J) 127/U), 374(1988)
13. Los Alamos Radiation Transport Group (X-6): LA-7396-M (1981)
14. ENDF/B summary documentation, BNL-NCS-17541, 3rd Edition (1979). C(MAT 1306, MOD 1) by C.Y. Fu and F.G. Perey (ORNL)